


# Green and scalable processing of water-soluble, biodegradable polymer/clay barrier films

Maximilian Röhrle<sup>1</sup> | Renee L. Timmins<sup>1</sup> | Dipannita Ghosh<sup>2</sup> |  
 Dominik D. Schuchardt<sup>1</sup> | Sabine Rosenfeldt<sup>3</sup> | Simon Nürnberger<sup>1</sup> |  
 Uwe Bölz<sup>4</sup> | Seema Agarwal<sup>2</sup> | Josef Breu<sup>1</sup> 

<sup>1</sup>Bavarian Polymer Institute, Department of Chemistry, University of Bayreuth, Bayreuth, Germany

<sup>2</sup>Macromolecular Chemistry II, Bavarian Polymer Institute, Department of Chemistry, University of Bayreuth, Bayreuth, Germany

<sup>3</sup>Physical Chemistry I, Bavarian Polymer Institute, Department of Chemistry, University of Bayreuth, Bayreuth, Germany

<sup>4</sup>HPX Polymers GmbH, Tutzing, Germany

## Correspondence

Josef Breu, Bavarian Polymer Institute and Department of Chemistry, University of Bayreuth, Bayreuth 95447, Germany.  
 Email: [josef.breu@uni-bayreuth.de](mailto:josef.breu@uni-bayreuth.de)

## Funding information

H2020 Marie Skłodowska-Curie Actions, Grant/Award Number: 860720; Deutsche Forschungsgemeinschaft, Grant/Award Number: SFB 1357-391977956

## Abstract

Poly(vinyl alcohol) (PVOH) based water-soluble packaging with intentional disposal into wastewater provides great convenience for both households and industry. In this paper, we demonstrate with CO<sub>2</sub> evolution testing that only insignificant fractions (~2%) of PVOH biodegrade in wastewater within 33 days. To avoid unintentional environmental build-up and the accompanying consequences to marine life, alternative materials with a suitable balance of performance and biodegradability are needed. Until now, the barrier properties of biodegradable biopolymers could not compete with state-of-the-art water-soluble packaging materials like PVOH films. In this paper, we report on waterborne, sandwich-structured films using hydroxypropyl methylcellulose or alginate produced with an industrially scalable slot-die coater system. The inner layer of the film consists of a collapsed nematic suspension of high aspect ratio synthetic clay nanosheets that act as an impermeable wall. Such a film structure not only allows for barrier filler loadings capable of sufficiently reducing oxygen and water vapor permeability of alginate to 0.063 cm<sup>3</sup> mm m<sup>-2</sup> day<sup>-1</sup> bar<sup>-1</sup> and 53.8 g mm m<sup>-2</sup> day<sup>-1</sup> bar<sup>-1</sup>, respectively, but also provides mechanical reinforcement to the biopolymer films facilitating scalable processing. Moreover, the films disintegrated in water in less than 6 min while rapid biodegradation of the dissolved polymer was observed.

## KEYWORDS

biodegradable and water-soluble packaging, microplastic, oxygen and water vapor barrier, slot die coating, sustainability

## 1 | INTRODUCTION

Water-soluble packaging films provide premeasured convenience to the delivery of dishwasher and laundry detergents, pesticides, fertilizer, dyes, and cement additives.<sup>1</sup>

Maximilian Röhrle and Renee L. Timmins contributed equally to this study.

This is an open access article under the terms of the [Creative Commons Attribution-NonCommercial](https://creativecommons.org/licenses/by-nc/4.0/) License, which permits use, distribution and reproduction in any medium, provided the original work is properly cited and is not used for commercial purposes.

© 2023 The Authors. *Journal of Applied Polymer Science* published by Wiley Periodicals LLC.

They are designed to dissolve and be released into the environment during use—particularly into wastewater streams. Poly(vinyl alcohol) (PVOH) is the most commonly employed polymer for such packaging as it is widely accepted as biodegradable. However, the kinetics of degradation in conventional wastewater are so slow that PVOH is actually considered a recalcitrant pollutant.<sup>2</sup>

Removal of PVOH from industrial wastewater is not accomplished through standard procedures, which consist of biological treatment with microbial stems that are commonly encountered in communal sewage plants to break down organic matter contaminants. The persistence of PVOH has led some to suggest the addition of advanced oxidation processes (ozonation, persulfate oxidation, electrochemical oxidation, etc.) to wastewater treatment facilities to reduce the level of contamination.<sup>3–5</sup> Unfortunately, this suggestion does not address the root of the problem and overlooks the poor worldwide accessibility to state-of-the-art wastewater treatment facilities.

Certain microorganisms, such as *Pseudomonas* (Sphingomonads) strains, are capable of biodegrading PVOH after acclimating in heavily contaminated waters, but the conditions for sufficient acclimation are highly specific. Such wastewater streams are primarily those of paper and textile treatment plants that continuously expel PVOH in large quantities.<sup>2,6,7</sup> Even with acclimated microorganisms, the kinetics of PVOH removal depends on various additional factors, including molecular weight, degree of hydrolysis, and the presence of salts.<sup>8,9</sup> PVOH contamination in natural water bodies has already brought consequences including increases in the chemical oxygen demand and inhibition of aerobic microorganisms, suffocating surface foam, and mobilization of heavy metals within water streams.<sup>5,10,11</sup>

Products that employ water-soluble films having an intentional disposal into the environment should be designed in a more responsible manner that does not contribute to wastewater pollution. The challenge is matching the excellent properties that PVOH provides with a more readily biodegradable alternative that meets the requirements during usage while allowing for being washed away. An ideal sustainable, water-soluble packaging film would exhibit biodegradability in wastewater, high gas barrier, flexible mechanical properties, transparent optical properties, as well as being suitable for high-volume manufacturing.

While natural biopolymers, including cellulose, alginate, whey protein, and so forth,<sup>12</sup> are quite attractive for use as alternative packaging material because they are readily water-soluble as well as biocompatible, nontoxic, and renewable,<sup>13</sup> they lack sufficient gas barrier and mechanical toughness. Both water vapor and oxygen barrier performance are critical considerations for commercial packaging

materials to prevent the breakdown of the film under ambient conditions and degradation of oxygen or water vapor sensitive products.<sup>14</sup> Some successful attempts to fabricate biopolymer films with properties relevant to water-soluble packaging offering a considerable water vapor barrier have been made at the lab scale, however, the fabrication techniques, including solvent casting or electrospinning, would not be practical for large-scale production.<sup>15,16</sup>

Improving the barrier of natural biopolymers can be accomplished effectively by the use of barrier fillers. The synthetic clay sodium hectorite (Hec) has imparted massive barrier improvements to biodegradable polymers in the past thanks to its exceptional aspect ratio and complete intercalation by water-soluble polymers.<sup>17,18</sup> Our group reported recently that band-like aggregates of Hec, even without an intercalated polymer matrix, provide an excellent barrier to oxygen due to the perfect clay nanosheet alignment induced during application by slot die coating.<sup>19</sup>

Slot die coating is a relatively unexplored lab-scale film preparation method that can easily be translated into a large-scale and low-cost roll-to-roll process. The instrument uses a die head having a thin slot from which metered solution exits onto a moving substrate. The encountered shear thinning on the applied solution is particularly useful to improve barrier properties due to the alignment of polymer chains and suspended barrier filler in the resulting film.<sup>20,21</sup>

In this work, we report a slot die coating method that can be translated into large-scale roll-to-roll manufacturing of high-barrier, self-standing biodegradable films for water-soluble packaging applications. Waterborne layered films made of Hec with either PVOH, hydroxypropyl methylcellulose (HPMC), or sodium alginate (alginate) were evaluated as a packaging material in terms of water solubility, gas barrier properties, mechanical performance, and optical properties. CO<sub>2</sub> evolution of the layered films in wastewater is compared to the same polymer film without Hec to ensure improvements in physical properties do not come at a sacrifice to biodegradability.

A roll-to-roll process easily enables the incorporation of multiple functional layers, unlike traditional solvent casting which is practically limited to a single monolayer. The layered structure of these films prevents complications that come with compounding a nematic Hec suspension with biopolymers like high viscosities, aggregation of filler, or embrittlement that limits high clay loadings.<sup>19</sup> At the same time, the exceptional barrier enhancement expected from the use of high aspect ratio nanosheets is ensured, producing biodegradable, high-performance, and scalable packaging films. With water being the only solvent employed, the production of the films aims to fulfill the 12 Principals of Green Chemistry.<sup>22</sup>

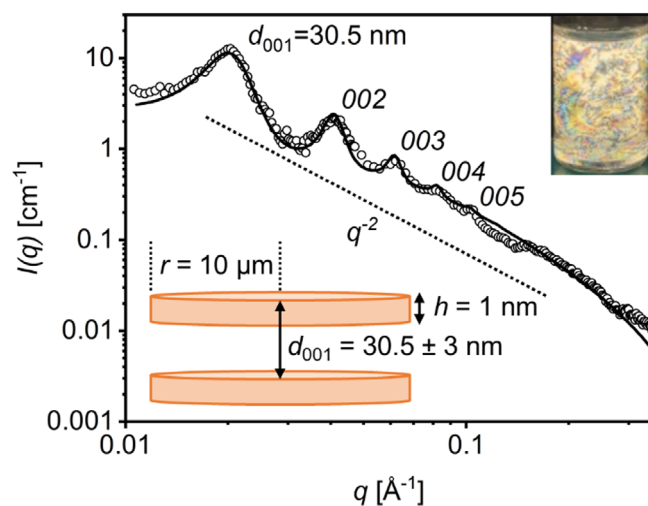


**FIGURE 1** Small angle x-ray scattering (SAXS) pattern of a 6 wt% ( $\approx 2.3$  vol%) aqueous Hec suspension with nanosheets uniformly separated to 30.5 nm ( $\circ$  measured,  $-$  calculated). The top inset shows birefringence of the diluted nematic Hec suspension between crossed polarizers. The bottom inset displays the model of disks used for the calculated SAXS intensity. [Color figure can be viewed at [wileyonlinelibrary.com](http://wileyonlinelibrary.com)]

## 2 | RESULTS AND DISCUSSION

### 2.1 | Film fabrication

A quantitatively delaminated suspension of Hec can be prepared by simply mixing the bulk clay in water. The rare phenomenon of thermodynamically allowed one-dimensional dissolution (i.e., osmotic swelling) that is accessible to this material provides single layers of negatively charged nanosheets without the use of mechanical force.<sup>23</sup> Fully delaminated Hec nanosheets have a preserved platelet diameter of  $\approx 20,000$  nm with a single layer thickness of 1 nm, yielding an exceptionally large aspect ratio (ratio of platelet diameter to thickness).<sup>24</sup> Such a high aspect ratio of  $\approx 20,000$  hinders rotation of adjacent Hec nanosheets in solution even at concentrations as low as 1 vol%,<sup>25</sup> giving a nematic liquid crystalline phase as indicated by the birefringence observed under cross-polarized light (Figure 1, top inset). Under closer inspection employing small angle x-ray scattering (SAXS), we can confirm a highly ordered liquid crystal structure with single Hec nanosheets separated to 30.5 nm corresponding to a 6 wt% ( $\approx 2.3$  vol%) aqueous Hec suspension (Figure 1). The  $q^{-2}$ -dependence of the SAXS curve at the low and intermediate  $q$ -range is characteristic for platy two-dimensional objects.<sup>26</sup> This geometry is further corroborated by applying a calculated model of disks with a radius of 10,000 nm ( $\pm 15\%$ ) and a thickness of 1 nm ( $\pm 7\%$ ) separated to a  $d$ -spacing of

$30.5 \pm 3$  nm using a Gaussian distribution (Figure 1, bottom inset). Observable reflexes up to 005 and an absence of peaks in the high  $q$  region that would indicate an undelaminated fraction verifies the presence of a translationally homogeneous nematic phase. The nematic nature of the Hec suspension is a critical aspect to obtain superior barrier properties since coated Hec nanosheets should lie parallel to the substrate and perpendicular to the direction of gas diffusion.<sup>27</sup> Retention of this structural order during processing will be ensured by employing a slot die coating instrument.

Separate polymer solutions of PVOH, HPMC, and Alginate were prepared by mixing the respective polymers with the plasticizers sorbitol and glycerol in a weight ratio of 80/10/10 (polymer/sorbitol/glycerol) in water. Plasticizers were added to obtain soft and flexible films as required for single-serving pouch applications. Solution concentrations and wet-coat heights were adjusted to warrant viscosities appropriate for slot die coating.

Due to the repulsive nature of the nanosheets that constitute liquid crystalline, delaminated Hec, suspensions of this material are highly viscous even at solid contents as low as 3 wt%.<sup>28</sup> The Hec suspension was prepared as 6 wt% in double distilled water, reflecting the maximum viscosity processible with the in-house slot die coater.

The polymer blends and the Hec suspension were then applied sequentially onto a PLA carrier substrate using a slot-die coater. The choice of material for the carrier substrate is inconsequential, as it will be removed from the layered films prior to analysis. In a similar fashion to the production of commercial layered films, the lab-scale slot-die coater provides precise and programmable solution deposition to make customizable layer structures. For this work, we chose a sandwich structure consisting of three layers arranged as polymer/Hec/polymer. With this structure, a suitable Hec content can be added without the concern of increasing viscosity of the polymer solution into ranges unsuitable for processing, as would be the case when working with a single, combined polymer/Hec suspension. Unlocking filler restrictions also gives access to properties of biopolymer nanocomposites that are unattainable with a homogeneous blend. A sandwich structure produced on a large-scale roll-to-roll process would consist of three sequential slot die heads, separated by drying units, and a collecting roll to remove the film from the carrier substrate when the addition of layers is complete (Figure 2a).

In our current laboratory setup, we are limited to a single slot die head, so the roll-to-roll process is stimulated by drying coated layers with a lamellar airflow dryer, then exchanging the solution in the slot die and

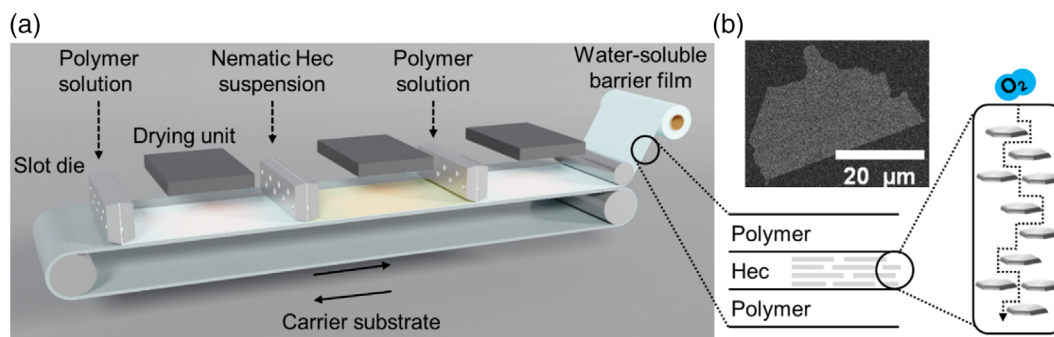


**FIGURE 2** (a) Sketch of the potential roll-to-roll processing method employing three consecutive slot die heads and drying units. In this way, a multi-layered film can be fabricated in-line and at high throughput by applying different coating solutions. Here we propose a layered sandwich structure with a first inner layer of water-soluble polymer, a second barrier layer of Hec and a third sealing layer of water-soluble polymer on top. The layered film is peeled-off and rolled-up while the carrier substrate can be reused. The inset highlights the tortuous path that a sandwiched Hec barrier layer provides against gas permeation. (b) Scanning electron microscopy (SEM) image of a single Hec nanosheet with a diameter  $>20\ \mu\text{m}$ . [Color figure can be viewed at [wileyonlinelibrary.com](http://wileyonlinelibrary.com)]

coating the next layer on top of the dry one. Given a desired dry film thickness and solution solid content, the wet coating thickness is adjusted by means of the pump flow rate, table speed, and coating gap. The final dry film can be easily peeled from the carrier substrate for analysis. A sandwich polymer film was produced from each of the three polymer solutions prepared. Due to the staggered stacking of platelets within a nematic Hec suspension and the large lateral extension of these sheets, we expect that the collapse of the structure upon drying will create a solid and nearly impermeable wall with a band-like structure and a diffusion path for permeates that is dramatically tortuous (Figure 2b).<sup>29</sup>

The final clay content of the PVOH, HPMC, and alginate layered films was determined from the residue that remains after a temperature ramp during thermal gravimetric analysis (Figure S1) as 21, 22, and 40 wt%, respectively. For comparison, monolayer films of each polymer (without Hec) were also prepared from the same polymer/plasticizer solution to ensure identical plasticizer content.

## 2.2 | Imaging

Cross-sections of each of the prepared films were observed with scanning electron microscopy (SEM) (Figure S2). The consecutive coating of individual layers provides highly uniform outer polymer layers of  $\approx 30\ \mu\text{m}$  sandwiching the inner Hec layer. The slight detachment of the top layer of polymer from the Hec layer is an artifact from preparation for imaging. The center Hec layer, which exhibits the proposed barrier wall structure, is  $\approx 6\ \mu\text{m}$  thick, neglecting the area of detachment. The ideal parallel alignment of the nanosheets can be attributed to the shear forces that

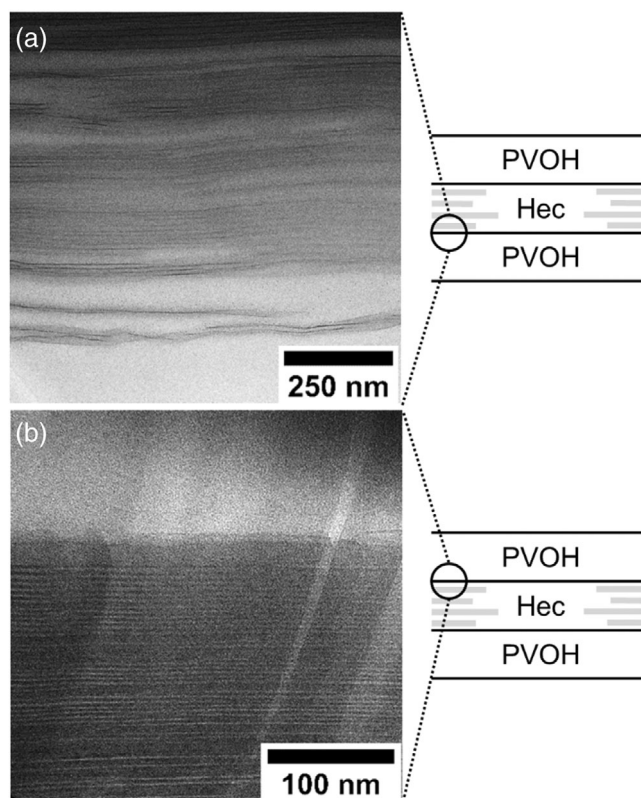


**FIGURE 3** Transmission electron microscope (TEM) cross-sections of the PVOH/Hec/PVOH film. (a) Interface between first PVOH sublayer and second Hec barrier layer. (b) Interface between second Hec barrier layer and top PVOH layer.

suspensions are subjected to within the slot die coating head, which retains the highly ordered, liquid crystalline Hec structure during processing.<sup>28</sup> Electron dispersive x-ray (EDX) element mapping of the film cross-sections with silicon from Hec represented in cyan and carbon from the PVOH represented in red aid in distinguishing the defined layer structure.

The layer interfaces within the PVOH/Hec/PVOH film were further investigated by transmission electron microscope (TEM) of the cross-sections prepared by cryo-ion-slicing (Figure 3). Observation of HPMC/Hec/HPMC and alginate/Hec/alginate films with TEM imaging was not possible as the ion beam used to prepare ultra-thin slices damages the biopolymers.

It appears that coating an aqueous Hec suspension onto the water-soluble PVOH sublayer leads to a partial re-dissolution of the dried polymer layer. This mobilizes the polymer, allowing it to diffuse between adjacent nanosheets that are separated to 30.5 nm in the liquid nematic state. The in-situ formed nanocomposite interface reaches only 1  $\mu\text{m}$  into the Hec layer due to the tortuosity imparted by the impermeable nanosheets that restrict further diffusion as drying progresses (Figure 3a). Such a structure at the interface provides excellent layer adhesion between the Hec and polymer domains. The amount of diffusion from the top layer of PVOH into the Hec region is less than the bottom layer of PVOH (Figure 3b), which explains its higher susceptibility to delayering as observed in the SEM image. Such behavior is not a surprise as a Hec layer is less prone to swelling upon removal of water and restacking of platelets. This suggests that the size of the nanocomposite interface could be modified by the drying treatment of the layers. Earlier studies have also demonstrated that the degree of PVOH intercalation into Hec can be modified by decreasing the drying temperature.<sup>20</sup>

The formation of an interfacial nanocomposite is assumed to form in the HPMC and alginate layered films as well due to their XRD patterns (Figure S3), which reflect a  $d$ -spacing of 1.6 and 1.4 nm, respectively. These values are substantially higher than the basal spacing of neat Hec ( $d_{001} = 0.96 \text{ nm}$ ).<sup>24</sup> The PVOH layered film also exhibits a  $d$ -spacing of 1.6 nm.

## 2.3 | Characterization and application

### 2.3.1 | Water solubility tests

The desired time for a water-soluble packaging film to disintegrate depends upon the mode of application. For household use, like in detergent pods, dissolution within minutes is desired, but it must be balanced with some degree of resistance to moisture or water vapor that may be encountered during transport and storage.

To evaluate film behavior when exposed to water, each film underwent water solubility testing according to the MSTM-205 testing standard (Figure S4). Films were held still in vigorously mixing water at room temperature. Disintegration time is defined as the time it takes until film breakage is observed, and dissolution time as

**TABLE 1** Disintegration and dissolution time of water-soluble films according to the method “MSTM-205 Solubility Test with Plastic Holder” in distilled water at a temperature of 23°C.

Film	Disintegration time (min)	Dissolution time (min)
PVOH/Hec/PVOH	5.7 $\pm$ 1.3	9.7 $\pm$ 2.1
HPMC/Hec/HPMC	5.9 $\pm$ 2.1	7.4 $\pm$ 2.1
Alginate/Hec/Alginate	2.9 $\pm$ 0.9	4.3 $\pm$ 0.6
PVOH	0.3 $\pm$ 0.1	0.4 $\pm$ 0
HPMC	0.3 $\pm$ 0.1	0.5 $\pm$ 0.1
Alginate	0.1 $\pm$ 0	0.1 $\pm$ 0

the time it takes until fragments of the film are no longer detectable by eye. Comparative tests were performed with neat polymer films (Table 1).

All of the plasticized polymer films exhibited disintegration in 0.3 min or less and underwent complete dissolution in no longer than 0.5 min, with HPMC taking the longest to do so. This is an expected result for these highly hydrophilic and water-soluble polymers. As a sandwich layered film, the time to disintegration was delayed to 2.9 min for alginate and 5.7 and 5.9 min for PVOH and HPMC, respectively. The time to disintegration, comparable to the time it would take for a pouch to release its contents, could be characterized for the desired application, for example, rapid release pouch (alginate film) or a standard release time (PVOH and HPMC film). Dissolution time of the three films ranged from 4.3 min for the alginate/Hec/alginate film to 9.7 min for the PVOH/Hec/PVOH film. The sandwich film structure proved able to provide some hydrophobicity when added to water-soluble polymers without totally hindering their ability to disintegrate rapidly. Hydrophobization has also been observed in intercalated Hec nanocomposites with other water-soluble polymers by means of an increased resistance to swelling and the improved water vapor barrier.<sup>17,30</sup> This slight modification of film properties makes them much more practical for real-world use where accidental exposure to water should not cause premature disintegration and exposure to humid conditions should not initiate excessive swelling that ruins film integrity and barrier. Films of the plasticized polymers themselves disintegrate within 20 s of exposure to water, which would lead to much wasted product if storage conditions are not strictly monitored. Although the layering of Hec within these same plasticized polymers increases their disintegration time, their ability to dissolve fully under 10 min at room temperature was not impeded. A range of disintegration and dissolution times could be customized by altering the film layer structure and by using different polymers to match expected packaging conditions.

Films/polymers	OP at 23°C and 50% RH (cm <sup>3</sup> mm m <sup>-2</sup> day <sup>-1</sup> bar <sup>-1</sup> )	WVP at 23°C and 85% RH (g mm m <sup>-2</sup> day <sup>-1</sup> bar <sup>-1</sup> )
PVOH/Hec/PVOH	0.008 (65% RH)	8.4
HPMC/Hec/HPMC	0.001 (65% RH)	12.5
Alginate/Hec/Alginate	0.063 (65% RH)	53.8
PVOH <sup>a</sup>	0.02 (0% RH)	1260
Poly(ethylene terephthalate) (PET) <sup>a</sup>	1–5	21–84
Polypropylene (PP) <sup>a</sup>	50–100	8–17
Polyethylene (PE) <sup>a</sup>	50–200	21–84
Poly(vinyl chloride) (PVC) <sup>a</sup>	2–8	42–84
Poly(lactic acid) (PLA) <sup>b</sup>	3–15 (0%/50% RH)	158–855
Poly(butylene adipate terephthalate) (PBAT) <sup>b</sup>	61	3450 (100% RH)
EVOH 32 mol% <sup>c</sup>	0.01 (65% RH)	-
Exceval <sup>d</sup>	0.002 (65% RH)	-

Note: Unless otherwise stated, the OP and WVP are given at test conditions of 23°C and 50% RH, 85% RH, respectively. Values are partially converted from their originally reported units allowing a consistent comparison.

<sup>a</sup>Lange and Wyser.<sup>31</sup>

<sup>b</sup>Wu et al.<sup>40</sup>

<sup>c</sup>Mitsubishi Gas Chemical.<sup>41</sup>

<sup>d</sup>Kuraray.<sup>32</sup>

### 2.3.2 | Gas barrier properties

Despite being water-soluble, the layered films provide exceptional protection against permeates, like oxygen and water vapor, that cause deteriorative reactions in many products. Oxygen transmission rate (OTR) and water vapor transmission rate (WVTR) values recorded for our layered films were converted into oxygen permeability (OP) and water vapor permeability (WVP) to normalize for film thickness and allow comparison across commercial and literature reports (Table 2). At a 65% relative humidity (RH), the PVOH, and HPMC layered films have an OP of 0.008 and 0.001 cm<sup>3</sup> mm m<sup>-2</sup> day<sup>-1</sup> bar<sup>-1</sup>, respectively. These values are comparable to the high-performance Exceval and outperform other common non-degradable packaging materials like polyethylene terephthalate (PET), polyethylene (PE), and poly(vinyl chloride) (PVC) measured at a lower 50% RH.<sup>31,32</sup> WVP values at a challenging 85% RH for PVOH and HPMC layered films are 8.4 and 12.5 g mm m<sup>-2</sup> day<sup>-1</sup> bar<sup>-1</sup>, respectively, once again outperforming the same commercial films.

While hydrophilic polymers like Exceval and ethylene vinyl alcohol (EVOH) swell at elevated RH, which degrades barrier performance,<sup>30,33</sup> the Hec barrier layer blocks diffusion of absorbed water and slows the swelling

TABLE 2 Oxygen permeability (OP) and water vapor permeability (WVP) of the water-soluble films compared with common polymers used for packaging and biodegradable polymers.

process. This becomes evident when comparing the WVP of 1260 g mm m<sup>-2</sup> day<sup>-1</sup> bar<sup>-1</sup> for neat water-soluble PVOH with the low WVP of 8.4 g mm m<sup>-2</sup> day<sup>-1</sup> bar<sup>-1</sup> found for the Hec loaded PVOH layered film at a demanding high 85% RH.<sup>31</sup> The incorporated Hec barrier layer hampers swelling and concomitant breakdown of barrier as indicated by a barrier improvement factor of 150.

Our processing strategy easily achieves top OP and WVP performance for HPMC among other HPMC systems reported in literature across various fillers and blends.<sup>34</sup> Although the layered alginate film falls slightly behind our other layered films and Exceval, it nevertheless outperforms several commercial packaging films and is competitive with the same materials in terms of WVP. The OP and WVP values for the alginate layered film of 0.063 cm<sup>3</sup> mm m<sup>-2</sup> day<sup>-1</sup> bar<sup>-1</sup> and 53.8 g mm m<sup>-2</sup> day<sup>-1</sup> bar<sup>-1</sup>, respectively, surpass previously reported barrier values for this material, even compared to other nanocomposites or crosslinked structures.<sup>35–39</sup> All of our layered films are orders of magnitude better in both OP and WVP when compared to commercial biodegradable films like PLA and poly(butylene adipate terephthalate) (PBAT). In general, the high barrier requirements for packaging are usually out of range for unfilled biodegradable materials.<sup>40</sup>

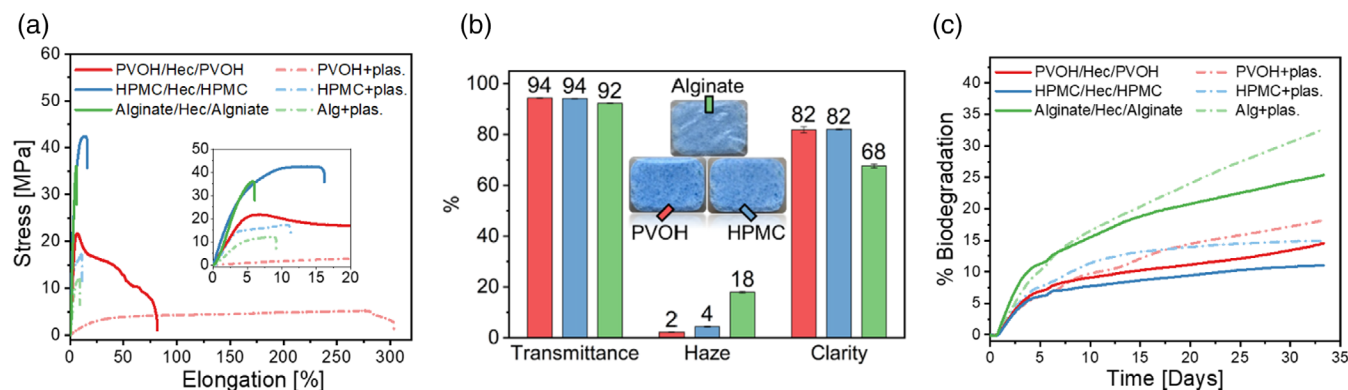


**FIGURE 4** Characterization of the films. (a) Mechanical properties of the plasticized polymers (10 wt% of each plasticizer, sorbitol, and glycerol) and their layered films with Hec. (b) Optical properties of layered films. (c) Biodegradation measured in terms of conversion to CO<sub>2</sub> of the plasticized polymers (10 wt% of each plasticizer, sorbitol, and glycerol) and their layered films with Hec. [Color figure can be viewed at [wileyonlinelibrary.com](http://wileyonlinelibrary.com)]

### 2.3.3 | Mechanical properties

With an excellent barrier to permeating gases, the evaluation of these layered films as a packaging material continues with the examination of mechanical performance. These water-soluble polymer layered films also exhibited excellent tensile properties suitable for flexible packaging films (Figure 4a, Table S1). The addition of the Hec layer improved the elastic modulus of all three of the plasticized polymers, establishing further functionality as a structural reinforcement. For alginate, the Hec layer boosts its elastic modulus from 35 to 1100 MPa. HPMC layered films exhibited nearly a 300% increase in its tensile strength. Naturally, percent elongation at break was reduced in all samples from the clay layer, however, severe embrittlement that is often observed in dispersed nanocomposite systems, even at much lower clay loadings than reported here, was avoided.<sup>38,42,43</sup> Moreover, the stretchability of PVOH is retained despite 22 wt% Hec, although delamination of the film layers was observed starting around 40% elongation.

A balance of suitable mechanical performance and suitable barrier properties has plagued degradable clay nanocomposites in the past due to how the same rigid, impermeable fillers that elongate the diffusion pathway for permeates also cause embrittlement of the polymer matrix.<sup>44</sup> These competing effects limited clay loading to below 5 wt% in dispersed nanocomposites and thus limited barrier performance. In this way, achieving high performance regarding both barrier and mechanical properties in a single material presented a huge hurdle to the implementation of biodegradable packaging materials with competitive performance. By the addition of common plasticizers and a sandwich-layered structure, we have evidently succeeded in mitigating

this embrittlement effect. The simple and scalable method of producing barrier films that we report here provides a promising solution to such critical hurdles of the past.

### 2.3.4 | Optical properties

Characterization of the optical properties of the layered films was performed to demonstrate how these films also meet the consumer preference for transparent packaging (Figure 4b). The PVOH layered film provides the most transparent film, while the alginate layered film suffers from slight haziness. Nevertheless, all three of the layered materials exhibit excellent optical properties that are suitable for transparent packaging needs, as displayed in an example of packaged dishwasher tablets (Figure 4b, inset).

### 2.3.5 | CO<sub>2</sub> evolution testing for biodegradation

Dissolution of polymers can favor biodegradation kinetics since, in the dissolved state, polymers have a maximized exposed surface area available to chain scission via hydrolysis. The oligomeric pieces may then be mineralized by microbial assimilation. However, this assimilation by microbes is not guaranteed simply by dissolution but additionally requires an appropriate match of enzymes and chain functionalities.

Therefore, the sandwich layered films and the plasticized polymer films were evaluated for their biodegradation in wastewater sludge by monitoring conversion into CO<sub>2</sub> for 33 days. Wastewater sludge was sourced from

the local wastewater treatment plant in Bayreuth, Germany. Cumulative CO<sub>2</sub> production was converted into percent biodegradation (Figure 4c), and aniline was used as the positive control. As additional references, the neat plasticizers were also evaluated under the same conditions (Figure S5). Sorbitol biodegraded 92% by the end of the 33 days, while glycerol degraded just 27% in the same time. With 10 wt% of each sorbitol and glycerol added to all films, we can therefore assume that ~12% of their total biodegradation in 33 days can be attributed to that of the plasticizers.

Taking a closer look at the biodegradation behavior of the plasticized polymer films reveals that PVOH and HPMC degradation reaches 14% and 11%, respectively. This biodegradation should be primarily, if not entirely, attributed to the plasticizers, exemplifying that although dissolved in water, these materials are incapable of degradation by microorganisms encountered in a typical communal sewage plant (or degrade too slowly to be non-persistent). As reported in the introduction, PVOH biodegradation requires a specialized environment with adapted microbes that are not common for communal sewage plants.<sup>2</sup> HPMC has shown to be biodegradable in soil,<sup>45</sup> however, this behavior is evidently not directly translatable to wastewater on a relevant timescale.

On the other hand, biodegradation on day 33 for the plasticized alginate and alginate/Hec/alginate of 33% and 25%, respectively, was recorded. Given that only 12% of the plasticizers would be assimilated at that point, the degradation of both the alginate samples substantially exceeds what could be attributed to the plasticizers. Clearly, alginate films are not only dissolved in freshwater but are also biodegraded in this wastewater environment.

Similarly to the dissolution kinetics, the biodegradation kinetics are slightly slowed down by the incorporation of a Hec layer into the center of the polymer films, likely attributed to its barrier effect. These biodegradation curves confirm that a sandwich-layered film with the barrier reinforcement material in the center provides optimal improvement in physical properties while also leaving the polymer accessible to biodegradation.

### 3 | CONCLUSION

Water-soluble packaging films provide unmatched convenience for dispensing both household and commercial products. In this work, we demonstrated the insignificant biodegradation of a commonly employed material, PVOH, in the disposal medium that it is designed for: wastewater. Similarly, and somewhat surprisingly, even a bio-based HPMC film showed no significant biodegradation, while the alginate films demonstrated up to 33% biodegradation

in 33 days. With rapid biodegradation and low production costs,<sup>46</sup> sodium alginate could make a viable commercial alternative to PVOH.

However, biopolymers, like alginate, cannot compete alone in demanding packaging applications due to their weak barrier and mechanical properties. By employing an industrially scalable slot die coating system (roll-to-roll processing), sandwich-structured films containing an inner hectorite clay barrier layer were obtained. This barrier layer could impart competitive properties to films of sodium alginate, including an OP and WVP of 0.063 cm<sup>3</sup> mm m<sup>-2</sup> day<sup>-1</sup> bar<sup>-1</sup> and 53.8 g mm m<sup>-2</sup> day<sup>-1</sup> bar<sup>-1</sup>, respectively. The layered film architecture, moreover, lifts previously encountered limitations on hectorite content related to rapidly increasing viscosity even at low filler contents. The shear-induced alignment of hectorite platelets during processing creates a highly ordered 6 μm thick impermeable barrier wall. An interfacial nanocomposite with the outer polymer layers that formed in situ during processing provided excellent layer adhesion and polymer confinement-induced barrier improvement. Possibilities of increasing the size of this nanocomposite area by varying the drying treatment have implications on further tuning interfacial adhesion, dissolution behavior, barrier properties, and possibly even mechanical properties to meet application-specific needs, which motivates a follow-up study.

## 4 | EXPERIMENTAL

### 4.1 | Materials and sample preparation

#### 4.1.1 | Materials

The synthetic clay sodium fluorohectorite (Hec) with the formula [Na<sub>0.5</sub>]<sup>inter</sup>[Mg<sub>2.5</sub>Li<sub>0.5</sub>]<sup>oct</sup>[Si<sub>4</sub>]<sup>tet</sup>O<sub>10</sub>F<sub>2</sub> was synthesized according to a published literature procedure and features a cation exchange capacity of 1.27 mmol g<sup>-1</sup>.<sup>24,47</sup> Poly(vinyl alcohol) (PVOH, Selvol 205, degree of hydrolysis 88%, ex Sekisui Chemicals Co., Japan), hydroxypropyl methylcellulose (HPMC, E15LV, ex Parchem Chemicals, United States), NaAlginat (alginate, Vivastar CS002, ex JRS, Germany), glycerol (CremerGLYC 3109921, ex Cremer Ole, Germany) and sorbitol (Neosorb<sup>®</sup> P 100 T, Roquette, France) were used without further purification. Biodegradable poly(lactic acid) (PLA, BoPLA-Folie NTSS 25 NT/25 μm, Pütz GmbH, Germany) films were used as substrates without further surface treatment.

#### 4.1.2 | Sample preparation

Hec was added to double-distilled water to obtain a 6 wt % Hec suspension. The suspension was placed for 7 days



in an overhead shaker to guarantee complete delamination into single Hec nanosheets.

One hundred grams of each of the three plasticized polymer suspensions (PVOH, HPMC, and alginate) were prepared by adding the polymer to double-distilled water in a round flask at 30 wt% for the PVOH, 20 wt% for the HPMC, and 15 wt% for the alginate suspension. The solid content was adjusted to achieve similar viscosities for slot die coating. The solutions were kept at 85°C under reflux for 2 h while stirring at 200 rpm using a magnetic stirring bar. Then the plasticizers were added to the polymer solutions so that the solid content of each was comprised of 80 wt% polymer, 10 wt% glycerol, and 10 wt% sorbitol.

### 4.1.3 | Slot die coating

The single water-soluble layers were produced consecutively by slot die coating (Table Coater equipped with a 1-Layer Slot Die 300 mm, AAA, TSE Troller AG, Switzerland). Prior to slot die coating, the polymer solutions and the Hec suspensions were homogenized, defoamed, and degassed under vacuum (50 mbar) for 5 min at 2500 rpm using a Speed-Mixer DAC 400.2 VAC-P (Hauschild, Germany). The applied shim ensures a coating width of 210 mm and a slot height of 165  $\mu\text{m}$ . The coating gap was adjusted according to the desired wet film thickness. The pump flow rate and the table speed were set accordingly depending on the coating gap. The vacuum table supported and fixed the PLA substrate needed for the first wet layer.

The table temperature, referred to as the drying temperature, was adjusted to the respective coated layer. The obtained wet films were dried in-line, generating a slight under pressure with an airflow of 1.5  $\text{m}^3 \text{min}^{-1}$ . The adjustable airflow was created by a Side Channel Blower Type 1SD 510 (Elektrot Airsystems GmbH, Germany). A micro-porous surface below the airflow guarantees a soft and uniform solvent removal over the entire wet film surface.

For details on the slot die coating settings applied for each layer, please refer to the Data S1. After drying was complete, the films were peeled off the PLA carrier substrate for analysis.

## 4.2 | Characterization methods

### 4.2.1 | Small-angle x-ray scattering

SAXS experiments were performed by employing the system Ganesha Air (SAXSLAB, Denmark). The system is equipped with a rotating anode copper x-ray source MicroMax 007HF (Rigaku Corp., Japan) and a position-

sensitive detector PILATUS 300K (Dectris, Switzerland) with adjustable sample-to-detector positions covering a wide range of scattering vectors  $q$ . The measurement of the suspension was conducted in 1 mm glass capillaries (Hilgenberg, Germany) at room temperature. The resulting one-dimensional (1D) data ( $I(q)$  [ $\text{cm}^{-1}$ ] vs.  $q$  [ $\text{\AA}^{-1}$ ], with intensity  $I(q)$ ) are background corrected and displayed in absolute scale.

The birefringence of a diluted Hec suspension was checked with a self-made crossed polarizer.

### 4.2.2 | Thermogravimetric analysis

Thermogravimetric analysis measurements were conducted on a Linseis STA PT 1600 (Linseis Messgeräte GmbH, Germany). The films were dried under vacuum ( $10^{-3}$  bar) at 70°C for 7 days. The dry samples were heated up from room temperature to 1000°C under an argon atmosphere with a heating rate of 10°C  $\text{min}^{-1}$ .

### 4.2.3 | Scanning electron microscopy

SEM images of a singular Hec nanosheet (Figure 2b) were recorded using the microscope ZEISS LEO 1530 (Carl Zeiss AG, Germany) operating at 3 kV and equipped with an InLens secondary electron detector. For sample preparation, the Hec suspension was diluted to 0.001 wt% and then drop-casted on a plasma-treated silicon wafer. Subsequently, the sample was sputtered with 1.2 nm of platinum.

SEM images of the cross-sections of the films were recorded using the microscope ZEISS Ultra plus (Carl Zeiss AG, Germany) operating at 5 kV and equipped with an InLens and secondary electron detector. The cross-sections were obtained by cutting the substrate-supported films with a scalpel toward the substrate side in order to protect the films. Subsequently, the films were carefully peeled off from the substrate. The film samples were sputtered with 1.2 nm of platinum. In addition, the cross-sections of the films were analyzed via EDX by employing an UltraDry-EDX detector (Thermo Fisher Scientific, United States).

### 4.2.4 | Transmission electron microscopy

TEM images of the cross sections were recorded employing a JEOL-JEM-2200FS (JEOL GmbH, Germany) microscope. Cross sections were prepared from the peeled-off films using a JEOL EM-09100IS Cryo Ion Slicer (JEOL GmbH, Germany).

#### 4.2.5 | X-ray diffraction

Diffraction patterns were obtained on a Bragg–Brentano-type instrument (Empyrean Malvern Panalytical BV, The Netherlands). The diffractometer is equipped with a PIXcel-1D detector, and Cu  $K_{\alpha}$  radiation ( $\lambda = 1.54187 \text{ \AA}$ ) was used. The patterns were analyzed by applying Malvern Panalytical's Highscore Plus software.

#### 4.2.6 | Water-solubility tests

The water-solubility of the films was tested according to the method "MSTM 205 Solubility Test with Plastic Holder." The setup is displayed in Figure S4. An average of three measurements for each film was taken.

#### 4.2.7 | Barrier properties

OTR were determined on the system OX-TRAN 2/21 (Mocon, United States) at 65% RH and 23°C. A mixture of 98 vol% nitrogen and 2 vol% hydrogen as carrier gas and pure oxygen (>99.95 vol%, Linde Sauerstoff 3.5) as permeant were used. WVTR were determined on the system PERMA-TRAN-W 3/33 (Mocon, United States) at 85% RH and 23°C. All samples were sufficiently equilibrated to guarantee moisture conditioning.

#### 4.2.8 | Coating thickness

The total film thickness was determined by employing High-Accuracy Digimatic Micrometer (Mitutoyo, Japan) with a measuring range of 0–25 mm and a resolution of 0.1  $\mu\text{m}$ . A mean value of 10 measuring points within the permeability measurement area of the film was taken.

#### 4.2.9 | Mechanical properties

Stress–strain tests were performed with a tensile instrument (Zwick/Roell, BT1-FR0.5TN.D14). The samples for the tensile measurement were cut to a size of 3 mm  $\times$  30 mm for a pristine effective tensile length of 10 mm. Prior to testing, the samples were equilibrated at 53% RH in a desiccator for 5 days. The test was performed with a crosshead speed of 5 mm  $\text{min}^{-1}$  at room temperature for at least 10 measurements. The slope of the linear region of the stress–strain curves was used to determine the elasticity modulus. All samples were measured at least 5 times, with the statistical average given as the result.

#### 4.2.10 | Optical properties

Optical properties were analyzed on a BYK-Gardner Haze-Gard Plus (BYK-Gardner GmbH, Germany). An average of five measurements per film sample were taken for transmittance, haze, and clarity values.

#### 4.2.11 | Biodegradation properties

The prepared films were tested for biodegradation in wastewater sludge under aerobic environment in triplicate for 33 days. The test method was based on DIN ISO 14851:2019. Activated sludge (after nitrification) collected from the wastewater treatment plant at Bayreuth, Germany, was used in the experiment as an inoculum. Aniline was used as the positive sample. Activated sludge in the same concentration was used as a control. Around 70 mg of the films were added in 100 mL test medium, with 95 mL of standard medium and 5 mL of supernatant of activated sludge. The Micro-Oxymax Respirometer furnished with a paramagnetic  $\text{O}_2$  and  $\text{CO}_2$  sensor (Columbus Instruments International, United States) was used for this biodegradation test.

The percentage of biodegradation was analyzed by observing the production of  $\text{CO}_2$  using the following equation:

$$\begin{aligned} \text{\%Biodegradation} &= \frac{(\text{mgCO}_2 \text{ produced})_{\text{T}} - (\text{mgCO}_2 \text{ produced})_{\text{B}}}{\text{ThCO}_2} \quad (1) \\ &\times 100 \end{aligned}$$

where  $(\text{mgCO}_2 \text{ produced})_{\text{T}}$  and  $(\text{mgCO}_2 \text{ produced})_{\text{B}}$  were the amounts of  $\text{CO}_2$  evolved in the test material and blank flask, respectively, given in milligrams.  $\text{ThCO}_2$  is the theoretical amount of  $\text{CO}_2$  expected to be evolved by the test material when completely mineralized and is calculated by:

$$\text{ThCO}_2 = \text{Specimen (mg)} \times \frac{\text{TOC (\%)}}{100} \times \frac{44}{12} \quad (2)$$

where 44 is the molecular weight of  $\text{CO}_2$  and 12 is the molecular weight of C, TOC (%) is the total carbon content of the test specimen determined by elemental analysis.

#### AUTHOR CONTRIBUTIONS

**Maximilian Röhl:** Conceptualization (lead); data curation (equal); methodology (lead); visualization (equal); writing – original draft (equal); writing – review and

editing (supporting). **Renee Timmins:** Conceptualization (equal); data curation (equal); methodology (supporting); visualization (equal); writing – original draft (equal); writing – review and editing (equal). **Dipannita Ghosh:** Formal analysis (supporting); methodology (equal); writing – review and editing (supporting). **Dominik Schuchardt:** Investigation (supporting); methodology (supporting); validation (supporting); writing – review and editing (supporting). **Sabine Rosenfeldt:** Data curation (supporting); methodology (supporting); software (equal); validation (supporting); writing – review and editing (supporting). **Simon Nürmberger:** Investigation (supporting); methodology (supporting). **Uwe Bölz:** Conceptualization (supporting); methodology (supporting); validation (supporting); writing – review and editing (supporting). **Seema Agarwal:** Funding acquisition (equal); project administration (equal); writing – review and editing (supporting). **Josef Breu:** Funding acquisition (lead); project administration (lead); supervision (lead); writing – review and editing (lead).

## ACKNOWLEDGMENTS

This study was funded by the Deutsche Forschungsgemeinschaft (DFG, German Research Foundation) – SFB 1357-391977956. This project has received funding from the European Union's Horizon 2020 research and innovation programme under the Marie Skłodowska-Curie agreement grant No. 860720. The authors cordially thank Florian Puchtler for producing the synthetic clay and Marco Schwarzmann for recording scanning and transmission electron microscope images. Furthermore, the authors are thankful for the support of the Keylabs for Optical and Electron Microscopy and Mesoscale Characterization: Scattering Techniques of the Bavarian Polymer Institute. Open Access funding enabled and organized by Projekt DEAL.

## CONFLICT OF INTEREST STATEMENT

The authors declare no conflict of interest.

## DATA AVAILABILITY STATEMENT

The data that support the findings of this study are available in the supplementary material of this article.

## ORCID

Josef Breu  <https://orcid.org/0000-0002-2547-3950>

## REFERENCES

- [1] T. A. Cooper, *Trends in Packaging of Food, Beverages and Other Fast-Moving Consumer Goods (FMCG)*, Woodhead Publishing, Cambridge, UK **2013**, p. 58.
- [2] N. Ben Halima, *RSC Adv.* **2016**, 6, 39823.
- [3] J. A. Giroto, R. Guardani, A. C. S. C. Teixeira, C. A. O. Nascimento, *Chem. Eng. Process.: Process Intensif.* **2006**, 45, 523.
- [4] C.-C. Lin, L.-T. Lee, *J. Ind. Eng. Chem.* **2015**, 21, 569.
- [5] W. Sun, L. Chen, J. Wang, *J. Adv. Oxid. Technol.* **2017**, 20, 20170018.
- [6] E. Chiellini, A. Corti, R. Solaro, *Polym. Degrad. Stab.* **1999**, 64, 305.
- [7] R. Solaro, A. Corti, E. Chiellini, *Polym. Adv. Technol.* **2000**, 11, 873.
- [8] E. Chiellini, A. Corti, S. D'Antone, R. Solaro, *Prog. Polym. Sci.* **2003**, 28, 963.
- [9] T. Vaclavkova, J. Ruzicka, M. Julinova, R. Vicha, M. Koutny, *Appl. Microbiol. Biotechnol.* **2007**, 76, 911.
- [10] S. Mondellini, M. Schott, M. G. Löder, S. Agarwal, A. Greiner, C. Laforsch, *Sci. Total Environ.* **2022**, 847, 157608.
- [11] H. Schonberger, A. Baumann, W. Keller, P. Pogopetris, *Am. Dyestuff Rep.* **1997**, 86, 9.
- [12] J. Nilsen-Nygaard, E. N. Fernández, T. Radusin, B. T. Rotabakk, J. Sarfraz, N. Sharmin, M. Sivertsvik, I. Sone, M. K. Pettersen, *Compr. Rev. Food Sci. Food Saf.* **2021**, 20, 1333.
- [13] G. A. Martău, M. Mihai, D. C. Vodnar, *Polymer* **2019**, 11, 1837.
- [14] K. K. Mokwena, J. Tang, *Crit. Rev. Food Sci. Nutr.* **2012**, 52, 640.
- [15] M. S. Abdel Aziz, H. E. Salama, M. W. Sabaa, *LWT* **2018**, 96, 455.
- [16] B. Akinalan Balik, S. Argin, J. M. Lagaron, S. Torres-Giner, *Appl. Sci.* **2019**, 9, 5136.
- [17] C. Habel, M. Schöttle, M. Daab, N. J. Eichstaedt, D. Wagner, H. Bakhshi, S. Agarwal, M. A. Horn, J. Breu, *Macromol. Mater. Eng.* **2018**, 303, 1800333.
- [18] J. Zhu, A. Kumar, P. Hu, C. Habel, J. Breu, S. Agarwal, *Global Chall.* **2020**, 4, 2000030.
- [19] R. L. Timmins, A. Kumar, M. Röhr, K. Havlíček, S. Agarwal, J. Breu, *Macromol. Mater. Eng.* **2022**, 307, 2100727.
- [20] M. Röhr, L. K. S. Federer, R. L. Timmins, S. Rosenfeldt, T. Dörres, C. Habel, J. Breu, *ACS Appl. Mater. Interfaces* **2021**, 13, 48101.
- [21] M. Röhr, J. H. Mettke, S. Rosenfeldt, H. Schmalz, U. Mansfeld, R. L. Timmins, C. Habel, J. Breu, F. Durst, *J. Coat. Technol. Res.* **2021**, 19, 487.
- [22] P. T. Anastas, J. C. Warner, *Green Chemistry: Theory and Practice*, Oxford University Press, Oxford, UK **1998**.
- [23] V. Dudko, O. Khoruzhenko, S. Weiß, M. Daab, P. Loch, W. Schwieger, J. Breu, *Adv. Mater. Technol.* **2022**, 8, 2200553.
- [24] M. Stöter, D. A. Kunz, M. Schmidt, D. Hirsemann, H. Kalo, B. Putz, J. Senker, J. Breu, *Langmuir* **2013**, 29, 1280.
- [25] S. Rosenfeldt, M. Stöter, M. Schlenk, T. Martin, R. Q. Albuquerque, S. Förster, J. Breu, *Langmuir* **2016**, 32, 10582.
- [26] L. Boldon, F. Laliberte, L. Liu, *Nano Rev.* **2015**, 6, 25661.
- [27] R. K. Bharadwaj, *Macromolecules* **2001**, 34, 9189.
- [28] M. Röhr, J. H. Mettke, S. Rosenfeldt, H. Schmalz, U. Mansfeld, R. L. Timmins, C. Habel, J. Breu, F. Durst, *J. Coat. Technol. Res.* **2022**, 19, 487.
- [29] E. L. Cussler, S. E. Hughes, W. J. Ward, R. Aris, *J. Membr. Sci.* **1988**, 38, 161.
- [30] T. Schilling, C. Habel, S. Rosenfeldt, M. Röhr, J. Breu, *ACS Appl. Polym. Mater.* **2020**, 2, 3010.

- [31] J. Lange, Y. Wyser, *Packag. Technol. Sci.* **2003**, *16*, 149.
- [32] Exceval™ – Attractive protection for your food. [https://www.kuraray-poval.com/fileadmin/technical\\_information/brochure\\_s/poval/Kuraray\\_Exceval\\_attractive\\_protection\\_for\\_your\\_food\\_engl.pdf](https://www.kuraray-poval.com/fileadmin/technical_information/brochure_s/poval/Kuraray_Exceval_attractive_protection_for_your_food_engl.pdf) (accessed: May 2023)
- [33] J. C. Grunlan, A. Grigorian, C. B. Hamilton, A. R. Mehrabi, *J. Appl. Polym. Sci.* **2004**, *93*, 1102.
- [34] R. Ghadermazi, S. Hamdipour, K. Sadeghi, R. Ghadermazi, A. Khosrowshahi Asl, *Food Sci. Nutr.* **2019**, *7*, 3363.
- [35] S. X. Weng, N. Yousefi, N. Tufenkji, *ACS Appl. Nano Mater.* **2019**, *2*, 1431.
- [36] M. Yang, Y. Xia, Y. Wang, X. Zhao, Z. Xue, F. Quan, C. Geng, Z. Zhao, *J. Appl. Polym. Sci.* **2016**, *133*, 43489.
- [37] H. Lee, B. Rukmanikrishnan, J. Lee, *Int. J. Biol. Macromol.* **2019**, *141*, 538.
- [38] M. Alboofetileh, M. Rezaei, H. Hosseini, M. Abdollahi, *J. Food Eng.* **2013**, *117*, 26.
- [39] S. Roy, J. W. Rhim, *Int. J. Biol. Macromol.* **2020**, *164*, 37.
- [40] F. Wu, M. Misra, A. K. Mohanty, *Prog. Polym. Sci.* **2021**, *117*, 101395.
- [41] Gas Barrier Properties. <https://www.mgc.co.jp/eng/products/ac/nmxd6/barrier.html> (accessed: September 2003)
- [42] A. A. Sapalidis, F. K. Katsaros, T. A. Steriotis, N. K. Kanellopoulos, *J. Appl. Polym. Sci.* **2012**, *123*, 1812.
- [43] K. E. Strawhecker, E. Manias, *Chem. Mater.* **2000**, *12*, 2943.
- [44] J.-W. Rhim, H.-M. Park, C.-S. Ha, *Prog. Polym. Sci.* **2013**, *38*, 1629.
- [45] C. G. Otoni, B. D. Lodi, M. V. Lorevice, R. C. Leitão, M. D. Ferreira, M. R. de Moura, L. H. Mattoso, *Ind. Crops Prod.* **2018**, *121*, 66.
- [46] O. Adeyeye, E. R. Sadiku, A. Babu Reddy, A. S. Ndamase, G. Makgatho, P. S. Sellamuthu, A. B. Perumal, R. B. Nambiar, V. O. Fasiku, I. D. Ibrahim, *Green Biopolymers and Their Nanocomposites*, Springer, Singapore **2019**, p. 137.
- [47] H. Kalo, M. W. Möller, M. Ziadeh, D. Dolejš, J. Breu, *Appl. Clay Sci.* **2010**, *48*, 39.

## SUPPORTING INFORMATION

Additional supporting information can be found online in the Supporting Information section at the end of this article.

**How to cite this article:** M. Röhr, R. L. Timmins, D. Ghosh, D. D. Schuchardt, S. Rosenfeldt, S. Nürnberger, U. Bölz, S. Agarwal, J. Breu, *J. Appl. Polym. Sci.* **2023**, *140*(37), e54418. <https://doi.org/10.1002/app.54418>